

## Low-lying levels of $^{57}\text{Mn}$ from the $^{54}\text{Cr}(\alpha, p)$ reaction\*

J. F. Mateja, G. F. Neal, J. D. Goss, P. R. Chagnon, and C. P. Browne

Department of Physics, University of Notre Dame, Notre Dame, Indiana 46556

(Received 14 October 1975)

Proton energy spectra from the  $^{54}\text{Cr}(\alpha, p)^{57}\text{Mn}$  reaction at 15, 21, and 24 MeV and at several angles have been measured with the 100-cm broad-range spectrograph. Both NaI(Tl) and Ge(Li) detectors have been used to study  $\gamma$  rays, in coincidence with protons in a particle detector, from the same reaction. From the spectrograph measurements, the ground-state  $Q$  value is found to be  $-4308 \pm 8$  keV. Excited levels have been found at  $84.1 \pm 1.0$ ,  $851.1 \pm 1.0$ ,  $1059.2 \pm 2.0$ ,  $1073.8 \pm 2.0$ ,  $1227.1 \pm 1.0$ ,  $1376.5 \pm 1.3$ ,  $2188.2 \pm 1.1$ , and  $2234.3 \pm 1.7$  keV. Ten  $\gamma$ -ray transitions have been observed. From particle- $\gamma$  coincidence and angular-correlation measurements the spins of some levels can be limited as follows: 84 keV,  $3/2-7/2$ ; 851 keV,  $3/2$  or  $5/2$ ; 1059 keV,  $1/2-5/2$ . Probable spin assignments for these three levels suggested on the basis of cross-section and relative transition-strength considerations are  $(7/2)$ ,  $(3/2)$ , and  $(1/2)$ , respectively. Other tentative spin assignments, and the comparison of  $^{57}\text{Mn}$  with other odd Mn isotopes, are discussed.

NUCLEAR REACTIONS  $^{54}\text{Cr}(\alpha, p)$ ,  $E = 15-24$  MeV; measured  $Q$ , levels.  
 $^{54}\text{Cr}(\alpha, p\gamma)$ ,  $E = 11.0-11.5$  MeV; measured  $p\gamma$ -coin,  $p\gamma(\theta)$ ,  $\gamma$  branching.  $^{57}\text{Mn}$   
 levels deduced  $J, \delta$ . Enriched target.

### I. INTRODUCTION

The low-lying levels of the odd Mn isotopes may be described, in terms of the spherical shell model, as primarily formed of three proton holes in the  $1f_{7/2}$  subshell. A comparison between  $^{53}\text{Mn}$  on the one hand and, on the other,  $^{51}\text{Mn}$  and  $^{55}\text{Mn}$  shows marked differences both in the level sequence and in electromagnetic transition rates.

The structure of  $^{53}\text{Mn}$ , which has 28 neutrons, is similar to that of other nuclei with three identical  $f_{7/2}$  particles or holes and one closed subshell, such as  $^{43,45}\text{Ca}$  and  $^{51}\text{V}$ . In these nuclei, the ordering of low-lying negative-parity levels among the spins allowed by the Pauli principle for the  $(\frac{7}{2})^3$  configuration is determined by the residual interactions among the valence particles.<sup>1-4</sup> The experimentally determined spin sequence begins  $\frac{7}{2}, \frac{5}{2}, \frac{3}{2}$  in each of these nuclei, in accord with calculations. Since  $M1$  transitions are forbidden between two states of the same  $(j)^n$  configuration, the large observed  $M1$  inhibitions, of the order of  $10^3$ , in these nuclei support this qualitative picture. For  $^{53}\text{Mn}$  in particular, Lips and McEllistrem<sup>4</sup> have carried out calculations with the  $(f_{7/2})^{-3}$  configuration extended to include excitation to the  $2p_{3/2}$  and  $1f_{5/2}$  subshells, which yield good quantitative agreement with experiment, both as to the level spectrum and as to transition rates.

The low-lying levels of  $^{51}\text{Mn}$  and  $^{55}\text{Mn}$ , while differing markedly from  $^{53}\text{Mn}$ , resemble each other and also resemble other nuclei such as  $^{47}\text{Ti}$  and  $^{49}\text{Cr}$  which have the  $(f_{7/2})^{+3}$  configuration with neither shell filled.<sup>5,6</sup> All of these nuclei have spin sequences beginning  $\frac{5}{2}, \frac{7}{2}, \frac{9}{2}, \frac{11}{2}$ , with  $M1$

transition rates among the low levels typically of the order of 0.1 Weisskopf unit. These characteristics can be reproduced by the rotational model with Coriolis coupling.<sup>7-10</sup> In these nuclei of relatively small mass the Coriolis effect is so strong as to alter significantly the level spacing expected in rotational bands, yet calculations which include the strong Coriolis coupling yield good qualitative agreement with experiment for a variety of such nuclei.

In particular, the close resemblance of  $^{55}\text{Mn}$  to  $^{51}\text{Mn}$  is easily accounted for according to this model, since only the deformation parameter would distinguish between them. In terms of the spherical shell model, the interactions between the proton holes and the valence neutrons or neutron holes have to be responsible for the structural differences between both  $^{51}\text{Mn}$  and  $^{55}\text{Mn}$ , and  $^{53}\text{Mn}$ . Since the dominant neutron configuration should be  $(2p_{3/2})^2$  in  $^{55}\text{Mn}$  and  $(1f_{7/2})^{-2}$  in  $^{51}\text{Mn}$ , the close similarity of these two to each other is unexpected from the shell model point of view.

In  $^{57}\text{Mn}$ , the subject of the present study, one might expect any of the following to occur. If adding two more neutrons relative to  $^{55}\text{Mn}$  merely alters the deformation parameter by a small amount, one would expect  $^{57}\text{Mn}$  to have the structure of  $^{51}\text{Mn}$ ,  $^{55}\text{Mn}$  and the other  $(f_{7/2})^{+3}$  nuclei with neither shell closed. But with the addition of two more neutrons the  $2p_{3/2}$  neutron subshell would be closed, in principle. If this closure is significant, then the  $^{57}\text{Mn}$  structure should closely resemble that of  $^{53}\text{Mn}$ , which also has a closed neutron subshell. Of course, if excitations of the valence neutrons are appreciable in the low-lying

states, the additional neutrons would have a pronounced effect on the low-lying level structure and  $^{57}\text{Mn}$  might not resemble either  $^{53}\text{Mn}$  or  $^{55}\text{Mn}$ .

From the  $\beta$  decay of the  $^{57}\text{Mn}$  ground state, its spin and parity have been established<sup>11,12</sup> as  $\frac{5}{2}^-$ . This would tend to indicate that  $^{57}\text{Mn}$  follows the pattern of the Mn isotopes with neither shell closed, rather than one shell closed.<sup>12</sup> No  $^{57}\text{Mn}$  excited levels were known at the inception of the present study.

## II. PROCEDURES

In this work,  $^{57}\text{Mn}$  was produced by the  $^{54}\text{Cr}(\alpha, p)$  reaction with  $^4\text{He}^{++}$  beams from the Notre Dame FN tandem Van de Graaff accelerator. First, reaction protons were momentum-analyzed with the Notre Dame 100-cm broad-range magnetic spectrograph in order to determine the ground-state  $Q$  value and the positions of the excited states. Runs were taken with the following incident  $\alpha$ -particle energies and laboratory observation angles: 15 MeV at 30°, 60°, and 90°; 21 MeV at 60°; and 24 MeV at 15°. Positive identifications of proton groups corresponding to levels in  $^{57}\text{Mn}$  were made with the aid of their kinematic shifts. The protons were detected by 50- $\mu\text{m}$ -thick Kodak NTA photographic plates mounted at the focal surface of the spectrograph. For these runs, targets approximately 20  $\mu\text{g}/\text{cm}^2$  thick were prepared by vacuum deposition of Cr metal enriched to 94.1% in  $^{54}\text{Cr}$  onto 20- $\mu\text{g}/\text{cm}^2$  carbon foils. Procedures for obtaining  $Q$  values and excitation energies from the spectrograph data were those described in earlier work.<sup>13</sup>

Particle- $\gamma$  coincidence spectra were taken in an axially symmetric geometry with the same reaction at beam energies of 11.0 and 11.5 MeV. Protons were detected near 180° with an 800- $\mu\text{m}$ -thick annular silicon surface-barrier detector. Elastically scattered particles were absorbed by a 10.6- $\text{mg}/\text{cm}^2$  Mylar foil covering this detector. Two types of  $\gamma$ -ray detectors were used. In one experiment five 10-cm $\times$ 10-cm NaI(Tl) detectors at different angles were operated simultaneously in coincidence with the protons. In another experiment, a 50-cm<sup>3</sup> Ge(Li) detector was placed alternately at 90° and 151° and also operated in coincidence with the protons. The  $\gamma$ -ray energy calibration sources were  $^{60}\text{Co}$ ,  $^{137}\text{Cs}$ , and  $^{182}\text{Ta}$ . Self-supporting targets approximately 160  $\mu\text{g}/\text{cm}^2$  thick had been prepared for these two experiments by vacuum evaporation of enriched  $^{54}\text{Cr}$  metal onto resistance-heated copper foils. The copper was then removed with a solution of ammonium hydroxide (50 cm<sup>3</sup>), trichloroacetic acid (10 g), and distilled water (50 cm<sup>3</sup>).

The axially symmetric reaction geometry, in conjunction with the zero-spin target and beam particles, permits only the  $M_J = \pm \frac{1}{2}$  magnetic substates of  $^{57}\text{Mn}$  to be populated in this experiment except for small contributions of other substates due to the finite size of the proton detector. The angular-correlation analysis of intensities from the NaI experiment followed conventional practice, with the population of  $M_J = \pm \frac{3}{2}$  magnetic substates limited to a maximum of 4% of the total, corresponding to the geometry of the experiment. A 0.1% confidence level was taken as the criterion for rejection of combinations of spin  $J$  and multipole mixing ratio  $\delta$ . The sign convention of Rose and Brink<sup>14</sup> is followed. Uncertainties in mixing ratio determined according to the method of Cline and Lesser<sup>15</sup> are quoted at the 95% confidence level.

Because the energies of some important  $\gamma$  rays lie below the threshold of the fast discriminators used in the NaI experiment, their angular correlations were not determined. It was thus necessary to extract the branching ratios from the Ge(Li) detector spectra. Data from the two detector angles in the Ge(Li) experiment were used to eliminate the second-order Legendre polynomial terms in the angular dependence. Possible fourth-order terms were neglected. Uncertainties in the branching ratios reported below are those due to counting statistics only.

## III. RESULTS

From the spectrograph data, the reaction  $Q$  value was determined to be  $-4308 \pm 8$  keV. This value is in agreement with the estimate of  $-4315 \pm 300$  keV reported by Maples, Goth, and Cerny.<sup>16</sup> There is a discrepancy of 138 keV between our results and the value of  $-4170 \pm 50$  keV calculated by Gove and Wapstra.<sup>17</sup> In calculating the  $Q$  value for this

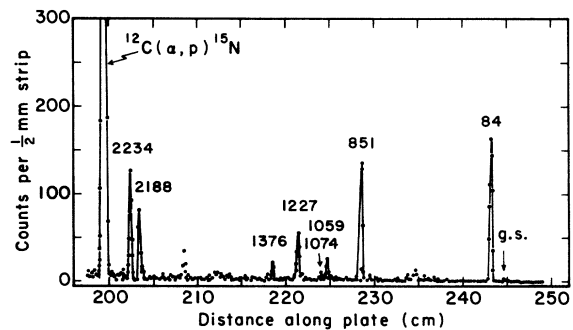


FIG. 1. Spectrum of protons from the  $^{54}\text{Cr}(\alpha, p)^{57}\text{Mn}$  reaction recorded with the 100-cm spectrograph. The bombarding energy was 24 MeV and the angle of observation was 15.5°. Groups are labeled with the excitation energy, in keV, in  $^{57}\text{Mn}$ .

TABLE I. Excitation energies determined with the magnetic spectrograph, and  $\gamma$ -ray branching ratios, of levels in  $^{57}\text{Mn}$ .

Initial level $E_x$ (keV)	Final level (keV)	Branching ratio
84.1 $\pm$ 1.0	0	(100) <sup>a</sup>
851.1 $\pm$ 1.0	0	100
1059.2 $\pm$ 2.0	0	12 $\pm$ 4
	851	88 $\pm$ 4
1073.8 $\pm$ 2.0	0	6 $\pm$ 6
	84	94 $\pm$ 6
1227.1 $\pm$ 1.0	84	94 $\pm$ 3
	1074	6 $\pm$ 3
1376.5 $\pm$ 1.3	84	72 $\pm$ 10
	851	28 $\pm$ 10
2188.2 $\pm$ 1.1		
2234.2 $\pm$ 1.7		

<sup>a</sup> The internal conversion coefficient of this transition is expected to be of the order of 4%.

reaction, Gove and Wapstra used the measured end-point energy of the  $\beta$  decay of  $^{57}\text{Fe}$  to the second excited state in  $^{57}\text{Mn}$ . It appears that they may have neglected to take into account the 136-keV excitation energy of this state in calculating the  $^{57}\text{Fe}$  to  $^{57}\text{Mn}$  ground-state energy difference. This correction would bring their value and the present measurement within quoted uncertainties. A pre-

liminary report of this result has been presented.<sup>18</sup>

One of the proton spectra taken with the magnetic spectrograph is presented in Fig. 1. A 4%  $^{52}\text{Cr}$  contaminant was responsible for most of the background in this spectrum. In general, the background was much more severe at the lower incident  $\alpha$ -particle energies. The  $^{54}\text{Cr}(\alpha, p)^{57}\text{Mn}$  cross sections were typically only 5% as large as those of  $^{52}\text{Cr}(\alpha, p)^{55}\text{Mn}$ . Data from five independent runs were averaged to obtain the excitation energies shown in the first column of Table I. The calculated excitation energy depends on the measured difference between the corresponding group and the ground-state group. The excitation energies, therefore, are not very sensitive to uncertainties in beam spot position, beam energy, angle of observation, and target stopping. The uncertainties in excitation energy were calculated according to the method of Jolivette *et al.*<sup>13</sup> These results constitute the first information on the excitation energies of  $^{57}\text{Mn}$ .

The placement of  $\gamma$  rays into the level scheme of  $^{57}\text{Mn}$  shown in Fig. 2 is based on the two-parameter  $p$ - $\gamma$  coincidence spectra in which each coincidence peak could be identified as to  $\gamma$ -ray energy and excited level. In the coincidence experiments with the NaI detectors, where the  $\gamma$ -ray energy resolution was poor, the problem of the  $^{52}\text{Cr}(\alpha, p\gamma)^{55}\text{Mn}$  background was compounded by small

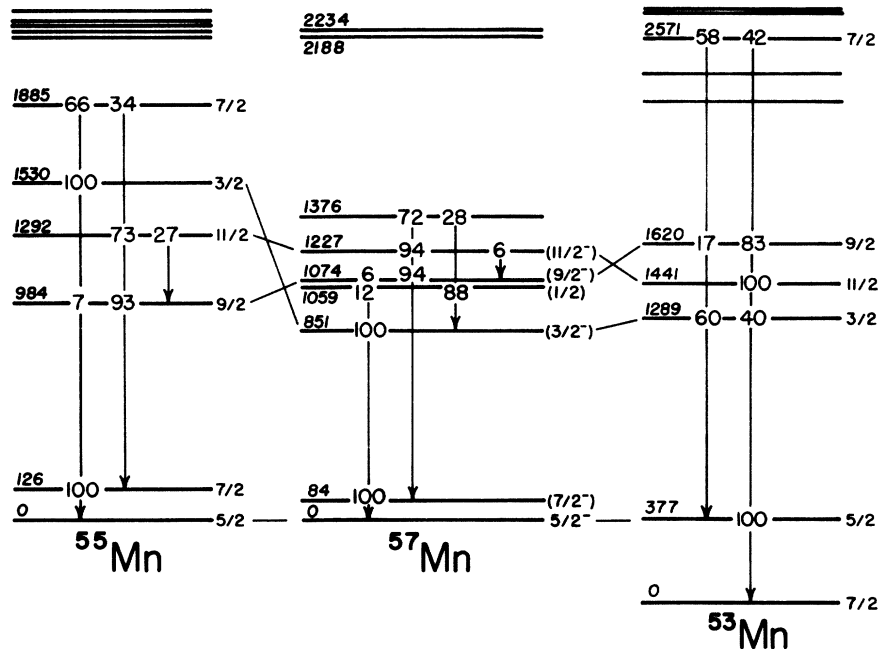


FIG. 2. Energy levels and branching ratios of  $^{57}\text{Mn}$  excited levels. Also shown are the low-lying levels of  $^{55}\text{Mn}$  taken from Ref. 6 and references therein, and those of  $^{53}\text{Mn}$  taken from Refs. 19 and 20. The lowest seniority-3 states of the three isotopes have been aligned; the arrows showing  $\gamma$ -ray transitions in  $^{53}\text{Mn}$  have been transposed so as to correspond to the same final-state spins as in the other two diagrams.

TABLE II. Minimum values of the normalized goodness-of-fit index  $\chi^2$  for 1, 3 correlation of the 851-keV  $\gamma$  ray coincident with protons feeding the 1059-keV level. The 0.1% confidence level falls at  $\chi^2 = 3.7$ . The full  $\chi^2$  plots for selected combinations of spins are shown in Fig. 4.

$J(851)$	$J(1059)$					
	$\frac{11}{2}$	$\frac{9}{2}$	$\frac{7}{2}$	$\frac{5}{2}$	$\frac{3}{2}$	$\frac{1}{2}$
$\frac{7}{2}$	15.4 <sup>a</sup>	10.7	7.2	6.0	6.5 <sup>a</sup>	
$\frac{5}{2}$		12.3 <sup>a</sup>	5.5	2.2 <sup>b</sup>	1.3 <sup>b</sup>	1.3
$\frac{3}{2}$			8.3 <sup>a</sup>	1.2 <sup>b</sup>	0.97	1.3

<sup>a</sup> Octupole-quadrupole mixture, arbitrarily cut off at  $\delta = \pm 0.5$ .

<sup>b</sup> Minimum occurs at quadrupole limit of quadrupole-dipole mixing.

chemical impurities of Cu and Mg. These impurities were probably introduced during the preparation of the self-supporting targets.

In the two-parameter  $p$ - $\gamma$  spectra taken with the NaI detectors, only two coincidence peaks were found to be sufficiently intense and free of contaminants to permit reliable angular-correlation analyses to be carried out. Figure 3 illustrates the analysis of the angular correlation of the 851-0-keV transition with protons feeding the 851-keV level. These results rule out (at the 0.1% confidence limit) the spin possibilities of  $\frac{9}{2}$  and  $\frac{1}{2}$ . From this angular correlation alone, the possible spins of the 851-keV level are  $\frac{3}{2}$ ,  $\frac{5}{2}$ , and  $\frac{7}{2}$ .

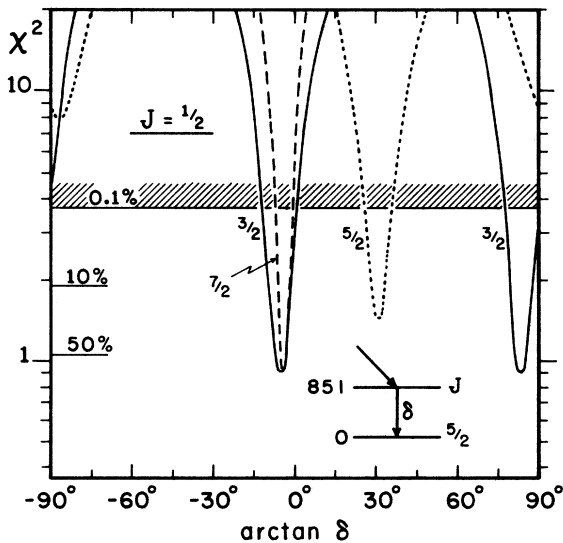


FIG. 3. The normalized goodness-of-fit parameter  $\chi^2$  plotted against the multipole mixing ratio  $\delta$  for the 851  $\rightarrow$  0-keV transition in  $^{57}\text{Mn}$ .

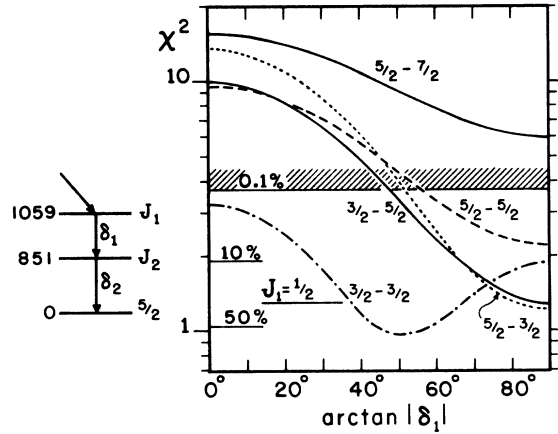


FIG. 4. Plot of  $\chi^2$  from the analysis of the 1, 3 correlation of the (1059  $\rightarrow$ ) 851  $\rightarrow$  0-keV sequence in  $^{57}\text{Mn}$ . The abscissa is the mixing ratio of the unobserved 1059  $\rightarrow$  851-keV transition. Mixing ratios  $\delta_2$  corresponding to the minima in Fig. 3 have been assumed for the 851  $\rightarrow$  0-keV transition. Where  $J_{851} = \frac{3}{2}$  has been assumed, either choice of  $\delta_2$  leads to the same  $\chi^2$  curves here. Other spin combinations are listed in Table II.

For the 1059-keV level, the low energy 1059  $\rightarrow$  851-keV  $\gamma$  rays did not trigger the coincidence circuit and the weak 1059  $\rightarrow$  0-keV transition was masked by the stronger 1073  $\rightarrow$  84-keV transition. The analysis of the 1, 3 angular correlation was carried out for the values of spins  $J_{1059}$  and  $J_{851}$  listed in Table II, with the mixing ratios  $\delta_2$  for the second transition corresponding to the minima in Fig. 3. For the case  $J_{851} = \frac{3}{2}$ , the two choices of mixing ratio produced nearly identical results. The  $\chi^2$  curves for selected combinations of spins are shown in Fig. 4. In all cases where  $J_{851} = \frac{1}{2}$  is assumed, the analysis of this 1, 3 correlation results in a  $\chi^2$  curve which fails to meet the 0.1% confidence limit. This eliminates the  $J = \frac{1}{2}$  possibility for the 851-keV level. All combinations of  $J_{851} = \frac{5}{2}$  or  $\frac{3}{2}$  with  $J_{1059} = \frac{1}{2}$ ,  $\frac{3}{2}$ , or  $\frac{5}{2}$  satisfy the 0.1%

TABLE III. Multipole mixing ratios corresponding to  $\chi^2$  minima in Figs. 3 and 4.

Transition (keV)	Assumed spins		Mixing ratio
	$J_i$	$J_f$	
851 $\rightarrow$ 0	$\frac{3}{2}$	$\frac{5}{2}$	$\delta = -0.1_{-0.4}^{+0.1}$ or $1/\delta = 0.1 \pm 0.1$
	$\frac{5}{2}$	$\frac{5}{2}$	$\delta = 0.60 \pm 0.15$
1059 $\rightarrow$ 851	$\frac{3}{2}$	$\frac{3}{2}$	$ \delta  = 1.2_{-1.0}^{+1.0}$
	$\frac{5}{2}$	$\frac{3}{2}$	$ 1/\delta  = 0.0 \pm 0.8$
	$\frac{3}{2}$	$\frac{5}{2}$	$ 1/\delta  = 0 \pm 1$
	$\frac{5}{2}$	$\frac{5}{2}$	$ 1/\delta  = 0.0 \pm 1.5$

confidence limit. All of these reach minima in  $\chi^2$  only at the quadrupole limit of quadrupole-dipole mixing except for the case  $J_{1059} = J_{851} = \frac{3}{2}$  and the case  $J_{1059} = \frac{1}{2}$ . In support of this last possibility, the intensities of the 208-keV  $\gamma$  ray from the 1059-keV level, as measured at  $90^\circ$  and  $151^\circ$ , were compatible with isotropic radiation within rather large statistical and systematic uncertainties of about 12%. The mixing ratios corresponding to minima in  $\chi^2$  for the 1059-851- and 851-0-keV transitions are listed in Table III.

#### IV. DISCUSSION

The energy levels and  $\gamma$ -ray transitions observed in  $^{57}\text{Mn}$  are presented in Fig. 2 along with portions of the level schemes of  $^{55}\text{Mn}$  and  $^{53}\text{Mn}$ . The 84-keV  $\gamma$  ray was observed with the Ge(Li) detector in 1, 2, and 1, 3 coincidences with protons feeding the 84-, 1074-, 1227-, and 1376-keV levels. Although the angular dependence is not accurately known and small numbers of counts prevailed, there was no perceptible loss of coincidence efficiency attributable to the lifetime of the 84-keV level. As the single-particle estimate of mean lifetime for an  $E2$  transition of 84 keV in  $A = 57$ , with an assumed 100-fold enhancement, is 150 ns, and the coincidence resolving time was 35 ns, we conclude that the 84-keV transition can be at most a dipole-quadrupole mixture. This limits the spin of the 84-keV level to  $\frac{3}{2}$ ,  $\frac{5}{2}$ , or  $\frac{7}{2}$ . The asymmetry of the 84-keV  $\gamma$  ray measured with the Ge(Li) detector is consistent with a spin of  $\frac{3}{2}$  or  $\frac{7}{2}$  if pure dipole radiation is assumed. This does not rigorously exclude a  $\frac{5}{2}$  spin, since a small but significant  $E2/M1$  interference is conceivable if the  $M1$  component is greatly retarded and the  $E2$  component enhanced.

The large relative intensity of the  $(\alpha, p)$  reaction to the 84-keV level in all of the spectra taken, including that in Fig. 1, suggests a direct process in which the proton in the transferred triton goes into an available  $f_{7/2}$  orbit. Since in the target nucleus the protons are coupled to  $J=0$ , such a direct transfer should favor population of a  $\frac{7}{2}^-$  state with single-proton character.

All of the known odd  $(f_{7/2})^3$  nuclei have a low-lying  $\frac{7}{2}^-$  level with a strong single-particle or seniority 1 component. In  $^{51}\text{Mn}$  it lies at 237 keV, and it lies at 126 keV in  $^{55}\text{Mn}$ . Thus all of the available evidence points to the  $\frac{7}{2}^-$  assignment for the 84-keV level in  $^{57}\text{Mn}$ . While rigorous proof is lacking, we propose this assignment provisionally.

In Fig. 2 we have included  $^{53}\text{Mn}$  (see Refs. 19 and 20), which may be called a closed-shell or spherical nucleus, and  $^{55}\text{Mn}$  ( $^{51}\text{Mn}$  is similar), which represents open-shell or rotational nuclei.<sup>6</sup> The figure has been prepared in such a way as to de-empha-

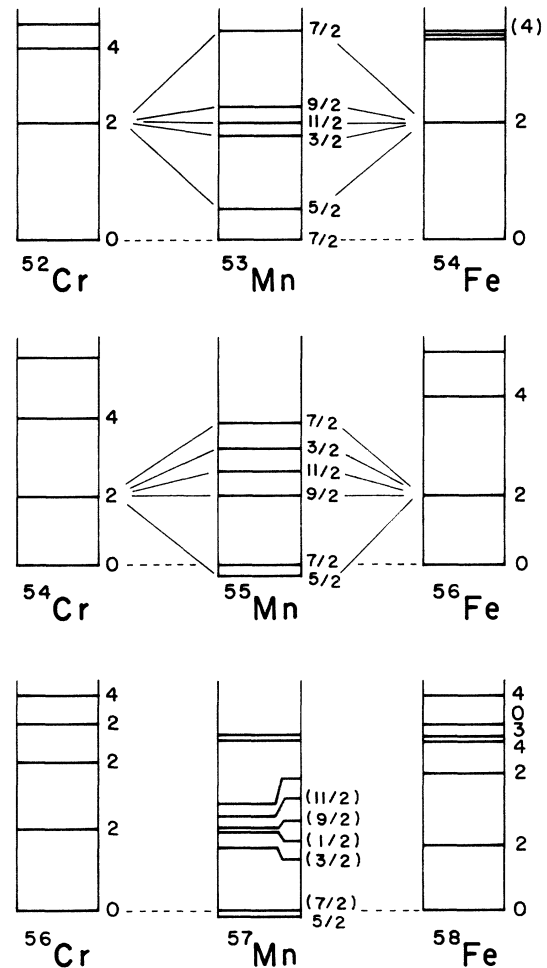


FIG. 5. Low-lying levels of  $^{53}\text{Mn}$ ,  $^{55}\text{Mn}$ ,  $^{57}\text{Mn}$  and of their even isotones. The easily recognizable  $\frac{7}{2}^- \otimes 2^+$  multiplet structure in  $^{53}\text{Mn}$  and  $^{55}\text{Mn}$  is obscured in  $^{57}\text{Mn}$ , at least by the presence of additional levels. Correspondingly, the first excited  $2^+$  level in  $^{56}\text{Cr}$  and  $^{58}\text{Fe}$  is not well isolated in comparison with the other even nuclei shown. Levels of the even nuclei are taken from Nuclear Data Sheets; additional information on  $^{56}\text{Cr}$  is from Ref. 21 and that on  $^{58}\text{Fe}$  is from Refs. 22 and 23.

size the differences among the better-known odd Mn isotopes and to bring out instead the similarity in certain low-lying states. These states could be thought of in an approximate sense as the multiplet  $(\frac{3}{2}^- \cdot \cdot \cdot \frac{1}{2}^-)$  formed by coupling a single  $f_{7/2}$  proton or hole to the  $2^+$  first excited level of the adjacent doubly even neighbor<sup>21-23</sup> of each Mn isotope (see Fig. 5). We do not propose that a single particle coupled to the core is a good representation for these states, but only use this scheme to identify the levels under discussion. In the lowest  $\frac{7}{2}^-$  state, in this terminology, the  $f_{7/2}$  proton or hole would be coupled to the  $0^+$  ground state of the neighbor. Putting aside the exact ordering of levels, one can

recognize common features among the isotopes in Fig. 2.

In both  $^{55}\text{Mn}$  and  $^{53}\text{Mn}$ , the  $\frac{11}{2}^- - \frac{7}{2}^-$  transition is prominent. (In  $^{55}\text{Mn}$  there is also a  $\frac{11}{2}^- - \frac{9}{2}^-$  branch which is not energetically possible in  $^{53}\text{Mn}$ .) Three levels in  $^{57}\text{Mn}$  are known to decay to the ( $\frac{7}{2}^-$ ) 84-keV state. Of these, neither the 1074- nor the 1376-keV levels can have spin  $\frac{11}{2}^-$  because of their transitions to the  $J = \frac{5}{2}^-$  ground state and to the  $J = \frac{5}{2}^-$  level at 851 keV. We therefore suggest that the 1227-keV level is the  $\frac{11}{2}^-$  state in  $^{57}\text{Mn}$ .

The weak branch 1227  $\rightarrow$  1074 keV, together with the decay of the 1074-keV level mainly to the  $\frac{7}{2}^-$  and more weakly to the  $\frac{5}{2}^-$  level, suggests that the 1074-keV level is the counterpart of the  $\frac{9}{2}^-$  levels in  $^{55}\text{Mn}$  and  $^{53}\text{Mn}$ . Of the remaining  $^{57}\text{Mn}$  levels in the group near 1 MeV, it is very unlikely that the 1376-keV level is the  $\frac{9}{2}^-$  level because it decays mainly to the  $\frac{7}{2}^-$  first excited state. Both the 851- and 1059-keV levels are possibly  $J = \frac{3}{2}^-$  states on the basis of the  $\gamma$ -ray transitions. The angular-correlation results already discussed, together with the strong branch 1059  $\rightarrow$  851 keV, which is energetically unfavored, and the 100% decay of the 851-keV level to the  $\frac{5}{2}^-$  ground state, strongly suggest that the 1059-keV level has  $J^\pi = \frac{1}{2}^-$  and that the 851-

keV level is the  $\frac{3}{2}^-$  state.

It has been pointed out<sup>3,6</sup> that the  $\frac{3}{2}^-$  level is subject to stronger configuration mixing than other levels, owing to the proximity of the  $2p_{3/2}$  orbit. This may be why the excitation energy of the  $\frac{3}{2}^-$  level exhibits more variation from one isotope to another than the higher-spin states. The lowest known  $J = \frac{3}{2}^-$  state in  $^{51}\text{Mn}$  is at 1825 keV.<sup>24</sup> If this is indeed the lowest  $\frac{3}{2}^-$  state, then there is a systematic decrease in excitation energy of the  $\frac{3}{2}^-$  state with increasing mass number from  $^{51}\text{Mn}$  to  $^{55}\text{Mn}$  to  $^{57}\text{Mn}$ .

It is evident that there are more levels near 1 MeV excitation in  $^{57}\text{Mn}$  than can be matched with the  $\frac{9}{2}^-$ ,  $\frac{11}{2}^-$ ,  $\frac{3}{2}^-$  group occurring in  $^{55}\text{Mn}$  and  $^{53}\text{Mn}$ . This is undoubtedly related to the number of low-lying states in the  $N = 32$  even isotones  $^{56}\text{Cr}$  and  $^{58}\text{Fe}$  (see Fig. 5). Already in  $^{52}\text{Cr}$  with 28 neutrons, configurations with neutrons excited to the  $2p_{3/2}$  orbit begin at about 2.7 MeV.<sup>4,25</sup> With 32 neutrons, there is a reduced energy gap for excitation of neutrons to  $2p_{1/2}$  and  $1f_{5/2}$  orbits; thus a multiplicity of low-lying low-spin states can be expected. It would appear that only a calculation in which not only the proton holes but also the neutrons are treated as valence particles will suffice to account for the low-lying structure of  $^{57}\text{Mn}$ .

\*Work supported in part by the National Science Foundation under grant No. GP-27456.

<sup>1</sup>I. Talmi, in *Proceedings of the Rehovoth Conference on Nuclear Structure*, edited by H. Lipkin (North-Holland, Amsterdam, 1958), p. 31.

<sup>2</sup>J. D. McCullen, B. F. Bayman, and L. Zamick, *Phys. Rev.* **134**, B515 (1964).

<sup>3</sup>R. A. Ricci, in *Nuclear Structure and Nuclear Reactions*, edited by M. Jean and R. A. Ricci (Academic, New York, 1969), p. 80.

<sup>4</sup>K. Lips and M. T. McEllistrem, *Phys. Rev. C* **1**, 1009 (1970); K. Lips, *ibid.* **4**, 1482 (1971).

<sup>5</sup>J. W. Noé, R. W. Zurmühle, and D. P. Balamuth, *Bull. Am. Phys. Soc.* **18**, 653 (1973); and (unpublished).

<sup>6</sup>B. P. Hichwa, J. C. Lawson, and P. R. Chagnon, *Nucl. Phys.* **A215**, 132 (1973).

<sup>7</sup>F. B. Malik and W. Scholz, *Phys. Rev.* **150**, 919 (1966).

<sup>8</sup>W. Scholz and F. B. Malik, *Phys. Rev.* **153**, 1071 (1967).

<sup>9</sup>R. W. Zurmühle, D. A. Hutcheon, and J. J. Weaver, *Nucl. Phys.* **A180**, 417 (1972).

<sup>10</sup>J. R. Comfort, P. Wasielewski, F. B. Malik, and W. Scholz, *Nucl. Phys.* **A160**, 385 (1971).

<sup>11</sup>K. G. Tirsell, L. G. Multhaus, and S. Raman, *Phys. Rev. C* **10**, 785 (1974).

<sup>12</sup>T. E. Ward, P. H. Pile, and P. K. Kuroda, *Nucl. Phys.* **A134**, 60 (1969).

<sup>13</sup>P. L. Jolivet, J. D. Goss, G. L. Marolt, A. A. Rollef-

son, and C. P. Browne, *Phys. Rev. C* **10**, 2449 (1974).  
<sup>14</sup>H. J. Rose and D. M. Brink, *Rev. Mod. Phys.* **39**, 306 (1967).

<sup>15</sup>D. Cline and P. M. S. Lesser, *Nucl. Instrum.* **82**, 291 (1970).

<sup>16</sup>C. Maples, G. W. Goth, and J. Cerny, LBL Report No. UCRL-16964, 1966 (unpublished).

<sup>17</sup>N. B. Gove and A. H. Wapstra, *Nucl. Data* **11**, 159 (1972).

<sup>18</sup>J. F. Mateja, G. F. Neal, J. D. Goss, P. R. Chagnon, and G. P. Browne, *Bull. Am. Phys. Soc.* **19**, 1337 (1974); and in *Proceedings of the Fifth International Conference on Atomic Masses and Fundamental Constants*, Paris, 1975 (Plenum, to be published).

<sup>19</sup>I. M. Szöghy, B. Čujec, and R. Dayras, *Nucl. Phys.* **A153**, 529 (1970).

<sup>20</sup>W. Chung, D. M. Sheppard, W. C. Olsen, and B. C. Robertson, *Can. J. Phys.* **51**, 1840 (1973).

<sup>21</sup>R. Chapman, S. Hinds, and A. E. MacGregor, *Nucl. Phys.* **A119**, 305 (1968).

<sup>22</sup>H. Schmidt, W. Michaelis, and U. Fanger, *Nucl. Phys.* **A136**, 122 (1969).

<sup>23</sup>G. Bruge, J. C. Faivre, H. Faraggi, and A. Bussière, *Nucl. Phys.* **A146**, 597 (1970).

<sup>24</sup>I. Forsblom, *Phys. Scr.* **6**, 309 (1972).

<sup>25</sup>S. W. Sprague, R. G. Arns, B. J. Brunner, S. E. Caldwell, and C. M. Rozsa, *Phys. Rev. C* **4**, 2074 (1971).